

Electroweak Effects in $e^+e^- \rightarrow \tau^+\tau^-$ at 29 GeV*

E. Fernandez, W. T. Ford, N. Qi, A. L. Read, Jr., J. G. Smith
Department of Physics
University of Colorado, Boulder, Colorado 80309

T. Camporesi, R. De Sangro, A. Marini, I. Peruzzi,
M. Piccolo, F. Ronga
Laboratori Nazionali Frascati dell' I.N.F.N., Italy

H. T. Blume, R. B. Hurst, J. P. Venuti, H. B. Wald, Roy Weinstein
Department of Physics
University of Houston, Houston, Texas 77004

H. R. Band, M. W. Gettner, G. P. Goderre, O. A. Meyer,^(a)
J. H. Moromisato, W. D. Shambroom, J. C. Sleeman, E. von Goeler
Department of Physics
Northeastern University, Boston, Massachusetts 02115

W. W. Ash, G. B. Chadwick, S. H. Clearwater,^(b)
R. W. Coombes, H. S. Kaye,^(c) K. H. Lau, R. E. Leedy,
H. L. Lynch, R. L. Messner, L. J. Moss,
F. Muller,^(d) H. N. Nelson, D. M. Ritson,
L. J. Rosenberg, D. E. Wiser, R. W. Zdarko
Department of Physics and Stanford Linear Accelerator Center
Stanford University, Stanford, California 94305

D. E. Groom, Hoyun Lee^(e)
Department of Physics
University of Utah, Salt Lake City, Utah 84112

M. C. Delfino, B. K. Heltsley,^(f) J. R. Johnson,
T. L. Lavine, T. Maruyama, R. Prepost
Department of Physics
University of Wisconsin, Madison, Wisconsin 53706

(Submitted to Physical Review Letters)

- (a) Present address: CERN, CH-1211, Geneva 23, Switzerland.
(b) Present address: Los Alamos National Lab., Los Alamos, NM 87545.
(c) Present address: Lawrence Berkeley Lab., Berkeley, CA 94720.
(d) Permanent address: CERN, CH-1211, Geneva 23, Switzerland.
(e) Present address: Department of Physics, Chungnam National University, Daejeon, Korea.
(f) Present address: Laboratory of Nuclear Studies, Cornell Univ., Ithaca, NY 14853.

*Work supported in part by the Department of Energy, under contract numbers DE-AC02-81ER40025 (CU), DE-AC03-76SF00515 (SLAC), and DE-AC02-76ER00881 (UW), by the National Science Foundation under contract numbers NSF-PHY83-08135 (UU), NSF-PHY82-15133 (UH), NSF-PHY82-15413 and NSF-PHY82-15414 (NU), and by I. N. F. N.

ABSTRACT

A high statistics measurement is presented of the cross section for the process $e^+e^- \rightarrow \tau^+\tau^-$ at $\sqrt{s} = 29$ GeV from the MAC detector at PEP. A fit to the angular distribution of our sample of 10153 events with $|\cos\theta| < 0.9$ gives an asymmetry $A_{\tau\tau} = -0.055 \pm 0.012 \pm 0.005$ from which we find the product of electron and tau axial-vector weak neutral couplings $g_A^e g_A^\tau = 0.22 \pm 0.05$.

PACS numbers: 13.10.+q, 12.30.Cx, 14.60.Jj

Although a number of experiments have provided precise measurements of the electron and muon axial-vector weak couplings,^{1,2} the couplings for the tau lepton are less well known. The forward-backward asymmetry of the reaction

$$e^+e^- \rightarrow \tau^+\tau^-(\gamma) \quad (1)$$

gives a direct measurement of this axial-vector portion of the weak neutral current and hence provides another important test of lepton universality. A measurement of the cross section for this process is obtained over 90% of the solid angle, from a large sample of data acquired with the MAC detector, operating at PEP at a center-of-mass energy of 29 GeV. The integrated luminosity for this sample is 210 ± 3 pb⁻¹.

The MAC detector, described in detail in ref. 3, includes a calorimeter/muon identifier of >95% solid angular acceptance. The calorimeter is composed of 91 cm of steel absorber surrounding the interaction point as a hexagonal prism with endcaps, with proportional wire chambers interspersed at 2.5 cm intervals to detect ionization from

traversing particles. The steel is magnetized by toroidal coils to about 1.8 T, and is surrounded by 4-6 layers of drift chambers for tracking muons. Inside the iron calorimeter is a lead plate shower chamber for detecting photon and electron showers in the central region, $|\cos\theta| \leq .8$; the inner portions of the endcap iron calorimeter serve the same function in the region $.7 \leq |\cos\theta| \leq .95$. Scintillators placed behind the electromagnetic calorimeters provide triggering and timing. Innermost is a ten-layer drift chamber inside a solenoid with a magnetic field strength of 0.57 T.

The trigger for the experiment consists of the logical OR of:

- (1) scintillator hits in opposite sextants or endcap quadrants;
- (2) scintillator hits on 3 or more of the 8 faces of the detector (modeled as a hexagonal prism);
- (3) showers of at least 2 GeV in any 2 of: 6 shower chamber sextants, 2 endcaps, or the central hadron calorimeter;
- (4) one or more penetrating tracks, defined by a cluster of central drift chamber hits within a 20° azimuthal sector in coincidence with a pulse of 400 MeV or greater in the matching calorimeter sextant and a signal in the corresponding scintillator(s).

About 50 million events passing an unrestrictive online filter were logged onto magnetic tape. An additional loose first-pass analysis filter rejects approximately 90% of these, leaving about 4 million (mostly Bhabha scattering) events for further analysis. A series of minimal cuts is then used in order to accept signal events down to small angles from the beam axis with high efficiency and low background. First, events are required to have at least two and not more

than four tracks (six in the case of events with reconstructed photon conversions in the beam pipe) reconstructed in the central drift chamber (CD); at least two of these tracks are required to have a satisfactory χ^2 for a primary vertex-constrained fit. The magnitude of the total charge for each event is required to be consistent with zero. A pair of tracks giving a satisfactory fit to the hypothesis of photon conversion in the beam pipe is not counted in the number of tracks for the cuts below (in order to treat these events like events with unconverted photons). Background from the process

$$e^+e^- \rightarrow \text{hadrons}, \quad (2)$$

is reduced by requiring one track to be separated from all others by at least 120° and the "jet" side to have no more than three charged tracks. Events with two tracks, both identified as muons or electrons, are rejected due to large backgrounds from the processes

$$e^+e^- \rightarrow \mu^+\mu^-(\gamma), \quad (3)$$

$$e^+e^- \rightarrow (e^+e^-)\mu^+\mu^-, \quad (4)$$

$$e^+e^- \rightarrow e^+e^-(\gamma), \quad (5)$$

$$e^+e^- \rightarrow (e^+e^-)e^+e^-, \quad (6)$$

as well as cosmic rays. This and the previous cut (eliminating events which have more than four charged tracks) reject only about 8% of events from process (1).

The total calorimetric energy is required to be greater than 6 GeV and electromagnetic shower energy to be less than about 23 GeV; the latter effectively rejects most Bhabha scattering events. Track quality cuts are made primarily to reduce the background from very low angle Bhabha events. To obtain further rejection of reaction (6) and radiative events from reactions (3) and (5), we eliminate events having an identified electron with an energy greater than about 5 GeV and a small angle from the beam axis, and events with neutrals which are consistent with a kinematic fit to an $ee\gamma$ or $\mu\mu\gamma$ hypothesis (including those with a photon conversion in the beam pipe). Further rejection of process (2) and beam-gas interaction events is achieved by requiring that the sphericity be less than 0.05 and the net transverse momentum relative to the thrust axis be less than 1.5 GeV/c. Events with tracks passing near the detector cracks or a single large spurious hit in the hadron calorimeters are rejected, mainly eliminating process (5). We veto events with several struck scintillation counters in each endcap, efficiently rejecting electrons, even near inactive regions of the calorimeter, since the scintillators are placed near shower maximum and their cracks do not coincide with those of the calorimeter. Events with the majority of tracks identified as electrons or muons are eliminated to reduce background from reactions (4) and (6).

To reduce backgrounds further, especially from process (5), several additional requirements are made on events with two charged tracks. They must be acollinear by more than 1° and acoplanar (the deviation of the two tracks from being back-to-back in the plane transverse to

the beam) by more than 1° and less than 40° . Also, to reduce cosmic ray and beam-gas backgrounds, the vertex requirement is tightened and the time difference between opposite struck scintillators is required to be consistent with tracks originating at the interaction point. Finally, several additional requirements are made of events which pass a track fit designed specifically for cosmic rays which miss the interaction point (especially along the beam direction).

In order to estimate the amount of background from processes (2)-(6), cosmic rays, and the reactions

$$e^+e^- \rightarrow (e^+e^-)\tau^+\tau^-, \quad (7)$$

$$e^+e^- \rightarrow (e^+e^-)\text{hadrons}, \quad (8)$$

we have altered some of the cuts most sensitive to the various backgrounds and used Monte Carlo calculations. The physics input for the latter relied on the calculation of Vermaseren et al.⁶ for processes (4) and (6)-(8), reference (5) for process (2) and reference (6) for the others. The detector simulation was performed using the full EGS⁷ (electromagnetic) and HETC⁸ (hadronic) shower codes and a detailed simulation of the physical and electronic properties of the various detector components of MAC. Finally, simulated events were processed by the same selection programs discussed above. These checks result in the following background estimates: (2) - 1.2%; (3) - 0.1%; (4) - 0.4%; (5) - <0.4%; (6) - 0.2%; (7) - 1.3%; (8) 0.4%; cosmic rays - 0.2%. The asymmetry is small for all of these processes except (5) for which it is nearly 100%; the only other significant source of an

asymmetry bias is process (4), where only one electron and one muon are detected, for which the total asymmetry bias is estimated to be 0.1%. The final sample contains 10153 events of which 400 ± 75 are background.

The standard electroweak theory⁹ prediction for production of tau pairs using unpolarized beams can be written, to first order in the Fermi coupling constant G , as

$$\frac{d\sigma}{d\cos\theta} = \frac{\pi\alpha^2}{2s} \left[(1+a_1)(1+\cos^2\theta) + 2a_2\cos\theta \right], \quad (9)$$

$$a_{1,2} = g^{eV,A} g^{\tau V,A} \frac{1}{\pi\alpha} \frac{G}{\sqrt{2}} \frac{-s}{1-s/M_Z^2},$$

where the center-of-mass energy is assumed to be small compared to the neutral vector boson mass M_Z , θ is the angle between the τ^+ and the incident positron, and the weak coupling constants g_A and g_V are predicted to be $-\frac{1}{2}$ and $\frac{1}{2}(4\sin^2\theta_W - 1) \approx -0.04$ respectively. The term proportional to $\cos\theta$, arising from the interference of the weak and electromagnetic amplitudes, results in the forward-backward (charge) asymmetry to which this experiment is sensitive. In order to compare this prediction with the data, it is necessary to correct for higher order QED processes, detector efficiency and backgrounds.

Radiative corrections are calculated with the Monte Carlo program of reference 6, including only diagrams to order α^3 . These diagrams give rise to a purely electromagnetic asymmetry which amounts to +1.8% after accounting for the cuts and acceptance. The Monte Carlo simula-

tion has been checked thoroughly with our radiative¹⁰ and non-radiative¹ muon pair production data.

To determine the overall detector and analysis efficiency, events simulating process (1) are produced. Taus are allowed to decay, using reasonably well-known branching ratios and proper decay matrix elements. These events are then passed through the detector simulation program discussed above. The resulting simulated events are processed by the same analysis programs as the data and a program simulating effects of the hardware trigger and online software filter. The inefficiency of this trigger is only 1.5% for events passing all other requirements. The overall analysis efficiency is determined by dividing the number of simulated events passing all cuts by the number of produced events for each bin in $\cos\theta$; the efficiency is $(42 \pm 1)\%$ when averaged over the acceptance and is nearly constant for all $|\cos\theta| < 0.7$. We define θ to be the angle between the thrust axis, taken in the direction of the positively charged "jet", and the direction of the incident positron; this prescription is unambiguous due to the event neutrality requirement mentioned above. The loss of information due to the imprecise knowledge of the tau direction ($\sigma_\theta = 3.5^\circ$) has a negligible effect on the analysis. Since the incorrect assignment of the charge of both jets happens in $< 1\%$ of the events, there is no significant dilution of the asymmetry.

The differential cross section shown in Fig. 1 is obtained after correction for the order α^3 radiative effects. All backgrounds discussed above are subtracted from the data bin-by-bin according to the

distribution of the Monte Carlo background events passing the cuts. A maximum-likelihood fit to (9) is performed in which a_2 and the normalization are varied (assuming $a_1 \ll 1$). The statistical and systematic errors in the background estimates are included in the fit. From this fit the charge asymmetry extrapolated to full acceptance is found to be

$$A_{\tau\tau} \equiv \frac{N_+ - N_-}{N_+ + N_-} = -\frac{3 a_2}{4(1+a_1)} = -0.055 \pm 0.012 \pm 0.005,$$

where the first error is statistical and the second systematic. The latter is dominated by the uncertainty in the background estimates for process (5). The fit gives a χ^2 of 21.8 for 16 degrees of freedom, with a normalization ($\sigma/\sigma_{\text{QED}}$) of $0.98 \pm 0.01 \pm 0.034$.

This result is considerably more precise than previous tau charge asymmetry measurements¹¹ and is in good agreement with the theoretical prediction of -0.063 at $\sqrt{s} = 29$ GeV and $M_Z = 90$ GeV. From the asymmetry and normalization given above, we find the weak coupling constants, $g_A^e g_A^\tau = 0.22 \pm 0.05$ and $g_V^e g_V^\tau = 0.06 \pm 0.10$. When combined with muon asymmetry results^{1,2}, these data provide good evidence for lepton universality.

We are grateful for the support of the SLAC staff and in particular the PEP operators, whose fine performance was responsible for the high statistics of this measurement.

References

1. E. Fernandez, et al., Phys. Rev. Letters 50,1238(1983); E. Fernandez, et al., SLAC-PUB-3133(1983).
2. W. Bartel, et al., Phys. Letters 108B,140(1982); B. Adeva, et al., Phys. Rev. Letters 48,1701(1982); M. E. Levi, et al., Phys. Rev. Letters 51,1941(1983); J. E. Kim, P. Langacker, M. Levine, and H. H. Williams, Rev. Mod. Phys. 53,211(1981).
3. MAC Collaboration, in "Proceedings of the International Conference on Instrumentation for Colliding Beams", edited by W. Ash, SLAC Report No. 250, 1982 (unpublished), p. 174; Roy Weinstein, in "American Institute of Physics proceeding No. 98, Particles and Fields subseries, No. 29" (Nov., 1982); Lawrence Berkeley Laboratory Report No. LBL-91 Supp., 1983.
4. R. Bhattacharya, J. Smith, and G. Grammer, Jr., Phys. Rev. D 15, 3267(1977); J. Smith, J. A. M. Vermaseren, and G. Grammer, Phys. Rev. D15,3280(1977).
5. T. Sjöstrand, Comput. Phys. Commun. 27,243(1982); T. Sjöstrand, Comput. Phys. Commun. 28,229(1983).
6. F. A. Berends, R. Kleiss, and S. Jadach, Nucl. Phys. B202,63(1982).
7. R. L. Ford and W. R. Nelson, SLAC-PUB-210(1978).
8. T. W. Armstrong in "Computer Techniques in Radiation Transport and Dosimetry", edited by W. R. Nelson and T. M. Jenkins (Plenum Press, New York, 1980).
9. S. Weinberg, Phys. Rev. Letters 19,1264(1967), and Phys. Rev. D 5, 1412(1972); A. Salam and J. C. Ward, Phys. Letters 13,168(1964); S. L. Glashow, Nucl. Phys. 22,579(1961).
10. W. T. Ford, et al., Phys. Rev. Letters 51,257(1983).

11. M. E. Levi, et al., Phys. Rev. Letters 51,1941(1983); R. Brandelik, et al., Phys. Letters 110B,173(1982); W. Bartel, et al., Phys. Letters 114B,282(1982); B. Naroska, in Proceedings of the International Symposium on Lepton and Photon Interactions at High Energies, edited by D. G. Cassel and D. L. Kreinick, Ithaca, N. Y., p. 96(1983).

Figure Caption

Fig. 1. Differential cross section for tau pair production, after radiative correction. The curve is the result of the fit described in the text.

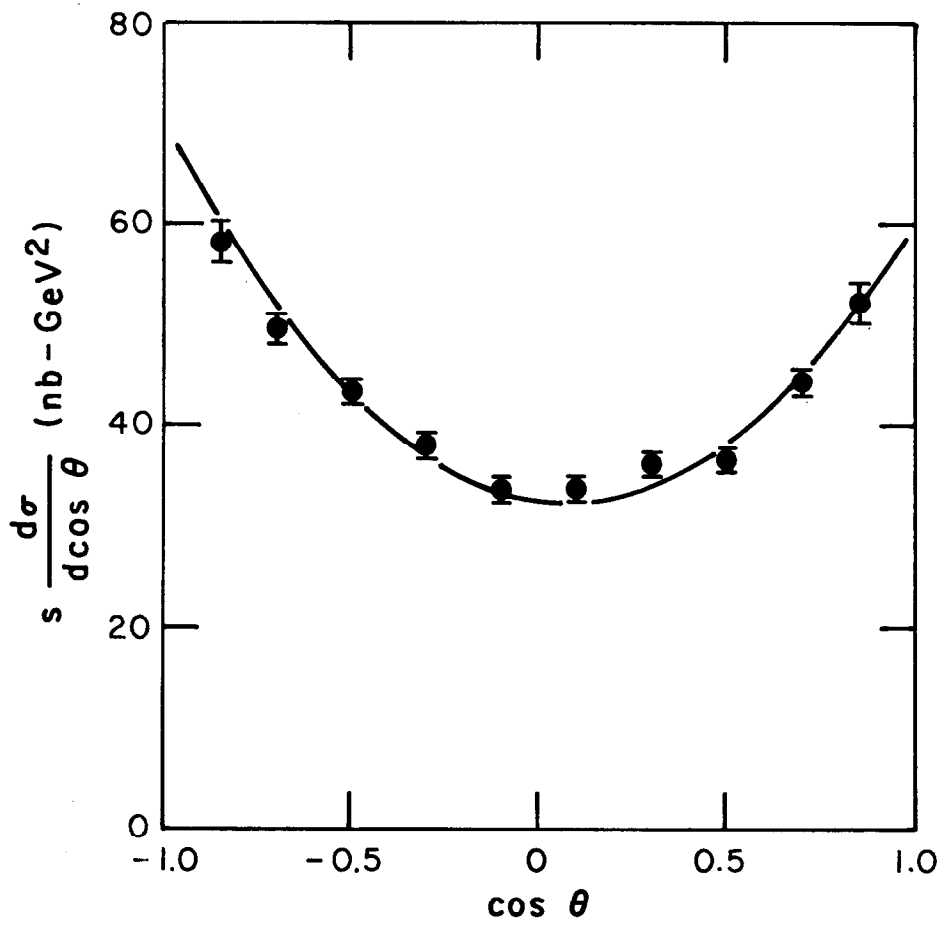


Fig. 1